



2 Responses of soil-mantled hillslopes to transient channel incision rates

3 Simon Marius Mudd¹ and David Jon Furbish²

4 Received 8 August 2006; accepted 6 September 2006; published XX Month 2007.

5 [1] Channel incision drives hillslope morphology in humid soil-mantled landscapes.
 6 When channel incision rates change, numerous hillslope soil properties (e.g., erosion rates,
 7 soil thickness, and soil production) adjust in response to this change. Here we investigate
 8 the timescales of adjustment of hillslope soil properties when channel incision rates
 9 change in time. An idealized soil-mantled hillslope (linear sediment flux law and soil
 10 density equal to bedrock density) is investigated, and the transient evolution of this
 11 hillslope is determined analytically. This analysis reveals two dominant adjustment
 12 timescales. The longer of these two timescales determines the rate at which the entire
 13 hillslope adjusts to a change in channel incision rates and is proportional to $4\lambda^2/(\pi^2 D)$,
 14 where λ is the length of the hillslope and D is the sediment diffusivity. Numerical
 15 simulations are then used to examine responses of hillslopes that involve nonlinear
 16 behavior (e.g., hillslopes that experience nonlinear sediment transport or have soil
 17 thicknesses that respond to the soil production function). Using these numerical models,
 18 we show that the ratio between the soil density (ρ_s) and the density of the soil parent
 19 material (ρ_η) can alter the long-term response of the hillslope such that the characteristic
 20 timescale becomes $4\rho_\eta\lambda^2/(\pi^2 D\rho_s)$. In addition, we show that the adjustments of the
 21 soil erosion rate, the soil production rate, and the soil thickness have different
 22 characteristic response timescales. Hillslopes that experience sediment flux that is
 23 proportional to the depth slope product respond on longer timescales than hillslopes that
 24 experience a linear sediment flux law when channel incision rates increase. We illustrate
 25 how the spatial pattern of hillslope response to changes in channel incision rates can
 26 be used to constrain either channel incision histories or hillslope response timescales. If
 27 the hillslope response timescale is known, the pattern of hillslope disturbance can be used
 28 to constrain the celerity of a incision wave as it moves upstream through a channel.
 29 If the channel incision history is known, the hillslope response timescale may be evaluated
 30 on the basis of the spatial pattern of hillslope disturbance.

31 **Citation:** Mudd, S. M., and D. J. Furbish (2007), Responses of soil-mantled hillslopes to transient channel incision rates, *J. Geophys.*
 32 *Res.*, 112, F03S18, doi:10.1029/2006JF000516.

34 1. Introduction

35 [2] The evolution of soil-mantled landscapes is driven, in
 36 part, by channels at the base of hillslopes that erode through
 37 the landscape and remove the sediment that is delivered to
 38 them by the hillslopes. The relationship between channel
 39 erosion rates and hillslope evolution has been a focus of
 40 geomorphic research for over a century [e.g., Davis, 1899;
 41 Gilbert, 1877; Hack, 1960; King, 1953; Penck, 1972].
 42 Modern understanding of the response of hillslope soils to
 43 changes in channel incision rates has followed the work of
 44 Culling [1960], who first applied a rigorous statement of
 45 mass conservation to an eroding hillslope soil.

[3] Gilbert [1909] suggested that the erosion rate of a 46
 hillslope soil is proportional to the topographic gradient, an 47
 observation that has been confirmed by a number of studies 48
 [e.g., Dietrich *et al.*, 2003, and references therein]. When 49
 channel incision rates change, several properties of the soil 50
 adjust in response. If, for example, the channel incision rate 51
 increases, the hillslope responds by steepening near the 52
 channel. As a result, soil thins near the channel. The 53
 steepening of the hillslope near the channel leads to removal 54
 of sediment upslope, thus removing soil at that location. In 55
 this way changes in channel incision rates result in changes 56
 in soil properties that propagate away from the channel 57
 [e.g., Furbish and Fagherazzi, 2001; Mudd and Furbish, 58
 2005; Roering *et al.*, 2001]. 59

[4] The adjustments of the soil to changes in channel 60
 incision rates exhibit characteristic timescales [e.g., Ahnert, 61
 1987; Fernandes and Dietrich, 1997; Furbish and 62
 Fagherazzi, 2001; Jyotsna and Haff, 1997; Roering *et al.*, 63
 2001]. These timescales include the time it takes the surface 64
 topography of the hillslope to adjust to a new channel 65
 incision rate (the hillslope relaxation time [e.g., Ahnert, 66

¹Department of Civil and Environmental Engineering, Vanderbilt University, Nashville, Tennessee, USA.

²Department of Earth and Environmental Sciences, Vanderbilt University, Nashville, Tennessee, USA.

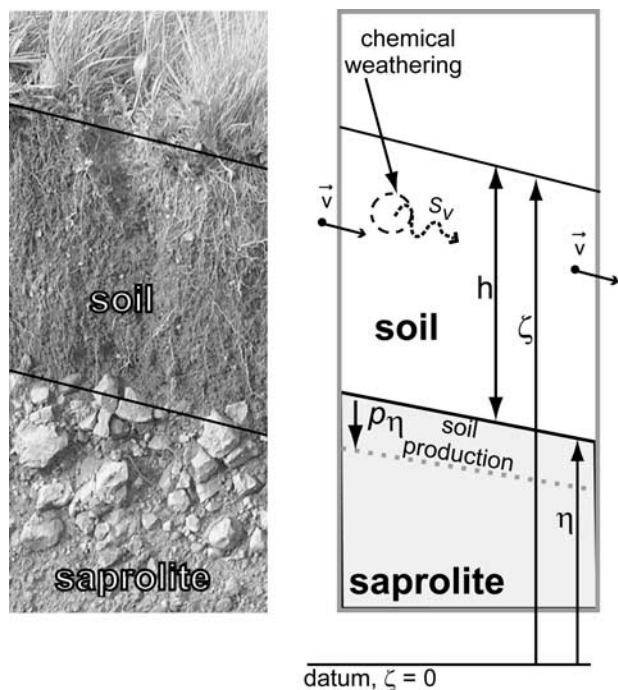


Figure 1. Schematic of the soil profile, where \bar{v} is the depth averaged bulk velocity of the sediment in the x direction, S_v is the mass loss rate per unit volume due to chemical weathering, h is the soil thickness, η is the elevation of the soil-bedrock boundary above an arbitrary datum, ζ is the elevation of the soil surface above an arbitrary datum, p_η ($L T^{-1}$) is the rate of bedrock lowering due to soil production, and the overbars denote depth-averaged quantities.

1987]), and the time needed for a perturbation in soil depth to propagate a specified distance upslope [e.g., Furbish and Fagherazzi, 2001].

[5] It is of fundamental importance to quantify these timescales for studies of both hillslope and fluvial geomorphology for two reasons. First, the timescale of transient hillslope response to changes in the channel incision rate provides an estimate of the period over which the resulting changes in soil properties are likely to persist on the hillslope, and thus is an estimate of the time a hillslope soil can record changes in channel incision rates. Second, the adjustment timescale of a hillslope soil responding to a change in channel incision rate must be known in order to evaluate whether it is appropriate to assume that a landscape has achieved a steady state or equilibrium condition. An equilibrium condition may be defined as the condition achieved when hillslope erosion rates have adjusted to match channel incision rates such that the surface topography of the landscape does not change in time and the landscape is lowering uniformly relative to base level [e.g., Carson and Kirkby, 1972; Gilbert, 1909; Hack, 1960; Howard, 1988].

[6] Here we extend the work of Fernandes and Dietrich [1997] and Roering et al. [2001], who examined the timescales over which hillslope soils respond to changes in channel incision rates, by including not only the response of hillslope erosion rates and surface topography but also the

soil thickness. For sufficiently simple conditions, the equations that govern the evolution of hillslope soils may be solved analytically. We report such solutions and use them to elucidate how hillslope soils respond to changes in channel incision rates. Namely, these solutions allow extraction of two timescales: one that can be used to estimate the adjustment rate of the entire hillslope to changes in channel incision rates and another that can be used to estimate the rate of propagation of the effects of transient channel incision as this signal moves away from the channel. In addition, we use numerical simulations to demonstrate that if channel incision rates are perturbed the response of different hillslope properties, such as the erosion rate, the soil thickness, and the soil production rate, will respond on different characteristic timescales. These different timescales can result in situations where, for example, the erosion rate of the hillslope may be equilibrated to a change in channel incision rate but the soil thickness may still be experiencing transient behavior.

2. Mass Conservation of Eroding Hillslope Soils

[7] We begin by considering soil-mantled landscapes in which the transport of soil due to landsliding and overland flow is insignificant. We define the soil layer as the near surface material that is being mechanically disturbed by processes such as soil creep [e.g., Culling, 1963; Heimsath et al., 2002; Kirkby, 1967; Roering et al., 1999; Young, 1978], animal burrowing and disturbance [e.g., Gabet, 2000; Yoo et al., 2005], frost heave processes [e.g., Anderson, 2002], and tree throw and root growth [e.g., Gabet et al., 2003; Roering et al., 2002]. In the presence of topographic gradients, this mechanically active layer is transported downslope. Underlying this mechanically active soil layer is a mechanically undisturbed saprolite layer. Material is entrained from the inactive saprolite into the active soil layer through soil production [e.g., Carson and Kirkby, 1972; Heimsath et al., 1997]. Once soil is produced, it can either accumulate locally or be removed through either mechanical or chemical denudation processes.

[8] Consider a one dimensional hillslope that has a mantle of soil with a thickness h (L), a surface elevation ζ (L) (Figure 1), and a soil-saprolite boundary that is at an elevation η (L) (Figure 1), such that the soil thickness is equal to:

$$h = \zeta - \eta. \quad (1)$$

A depth integrated [e.g., Mudd and Furbish, 2004; Paola and Voller, 2005] statement of mass conservation for the hillslope soil is

$$\frac{\partial h}{\partial t} = -\frac{\partial(h\bar{v}_x)}{\partial x} + \frac{\rho_\eta}{\rho_s} p_\eta, \quad (2)$$

where ρ_s ($M L^{-3}$) is the dry bulk density of the soil, v_x ($L T^{-1}$) is the bulk velocity of the sediment in the x direction, ρ_η ($M L^{-3}$) is the density of the parent material, p_η ($L T^{-1}$) is the rate of bedrock lowering due to soil production, and the overbars denote depth-averaged quantities. All terms in equation (2) represent rates of change in the soil thickness, in units of length per time. The first term on the right of the

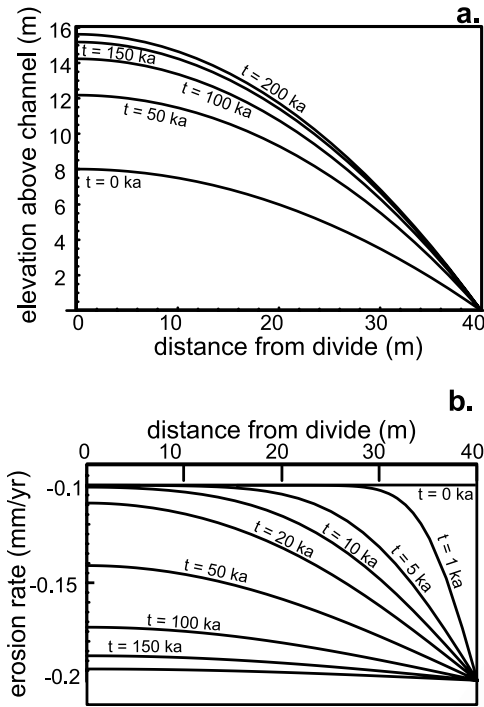


Figure 3. Analytical solutions of equation (6) for (a) surface topography and (b) erosion rate. The hillslope is 40 m long ($\lambda = 40$ m) and has a diffusivity (D) of $0.01 \text{ m}^2 \text{ yr}^{-1}$. Initially, the hillslope topography reflects a steady condition adjusted to a channel incision rate (I_0) of 0.0001 m yr^{-1} . At time $t = 0$ the channel incision rate is increased to 0.0002 m yr^{-1} .

230 presented by *Culling* [1965] in that we include an incising
 231 channel and our initial hillslope is adjusted to a down-
 232 cutting rate of I_0 . In contrast, *Culling* [1965] presented
 233 solutions for a hillslope whose channel stayed at a constant
 234 elevation such that the hillslope was eroded to a plane, and
 235 a hillslope bounded on both sides by channels that incised
 236 at a constant rate. The significance of the new derivation is
 237 that we are able to investigate the dynamics of hillslope
 238 adjustment to changes in channel incision rates rather than
 239 the time necessary to achieve a denuded, peneplane-like
 240 surface as investigated by *Culling* [1965].

241 [14] The local erosion rate of the hillslope soil as a
 242 function of time and space can be found by differentiating
 243 equation (7):

$$\frac{\partial \zeta}{\partial t} = -I - \frac{4}{\pi} (I_0 - I) \sum_{n=0}^{\infty} \frac{(-1)^n}{(1+2n)} e^{-\frac{D\pi^2(1+2n)^2 t}{4\lambda^2}} \cdot \cos \left[\frac{\pi(1+2n)x}{2\lambda} \right]. \quad (8)$$

245 Equation (8) is measured relative to a fixed datum (i.e., not
 246 relative to the incision rate of the channel). An example of a
 247 hillslope responding to a change in the rate of channel
 248 incision at its base as described by equations (7) and (8) is
 249 shown in Figure 3.

[15] *Howard* [1988] suggested that the adjustment of a
 hillslope to a step change in the channel incision rate can be
 approximated by an exponential decay function of the form

$$F(t) = F_f + (F_i - F_f)e^{-t/\tau}, \quad (9)$$

where F is a time dependant function, F_f is the value of the
 function at its final equilibrium value, F_i is the initial value
 of the function, and $\tau(T)$ is a timescale that characterizes the
 rate at which the transient signal decays (e.g., if $t = 3\tau$ the
 function is within 5% of the final equilibrium value). Both
Roering et al. [2001] and *Mudd and Furbish* [2005] used
 equation (9) to estimate hillslope response timescales, but as
 observed by *Mudd and Furbish* [2005], this approach may
 not be adequate to fully characterize the response timescales
 of soil-mantled hillslopes.

[16] Equation (9) may be used to fit values of the
 timescale of the hillslope response to changes in the channel
 incision rate (τ) at different points on the hillslope, and this
 fit may be compared with the precise timescale of response
 extracted from equation (8). Figure 4 shows a comparison
 of the precise erosion rate predicted by equation (8) and
 the erosion rate based on the simple exponential response
 described by equation (9) as a function of time. Near the
 channel, the hillslope responds rapidly to the perturbation
 of the channel incision rate (Figure 4b), whereas at points near
 the divide (Figure 4a) the perturbation is only felt after some
 delay (as identified by *Roering et al.* [2001] in their Figure 8).
 As time increases, equation (9) can approximate the response
 of the hillslope, but it does not capture the shorter timescale
 behavior that causes a fast response near the channel and a
 delayed response near the divide (Figure 4).

[17] As noted by *Culling* [1965] and embodied in equa-
 tion (7) and equation (8), the response of the hillslope can
 be described by a sum of harmonic functions. Each wave
 number (i.e., $n = 0, 1, 2, 3, \dots$) in the series of harmonic
 functions has a different characteristic timescale, analogous
 to τ in equation (9). The timescale for each harmonic
 function, $\tau_n(T)$, is

$$\tau_n = \frac{4\lambda^2}{D\pi^2(1+2n)^2}. \quad (10)$$

As the wave number increases, the characteristic timescale
 decreases, such that the long-term behavior of the hillslope
 is dominated by the wave number $n = 0$, or in other words,
 $\tau_0 = 4\lambda^2/(D\pi^2) = 0.4053\lambda^2/D$, which is equivalent to the
 relaxation timescale found numerically by *Roering et al.*
 [2001] for hillslopes whose sediment flux is a linear
 function of slope. The effect of different wave numbers on
 the erosion rate of a hillslope whose channel incision rate
 has been perturbed is plotted in Figure 5.

[18] Because signals propagate away from the channel,
 the transient response of the hillslope due to the effects of
 higher wave numbers (i.e., $n > 0$) varies as a function of
 distance from the channel (Figure 5). Near the channel
 (Figure 5b), the effect of the harmonics with higher wave
 number (e.g., $n > 0$) combine to cause the hillslope to
 respond rapidly to the change in the rate of channel incision;
 this rapid incision is not captured by equation (9) (see
 Figure 4b). On the other hand, the effect of the harmonics

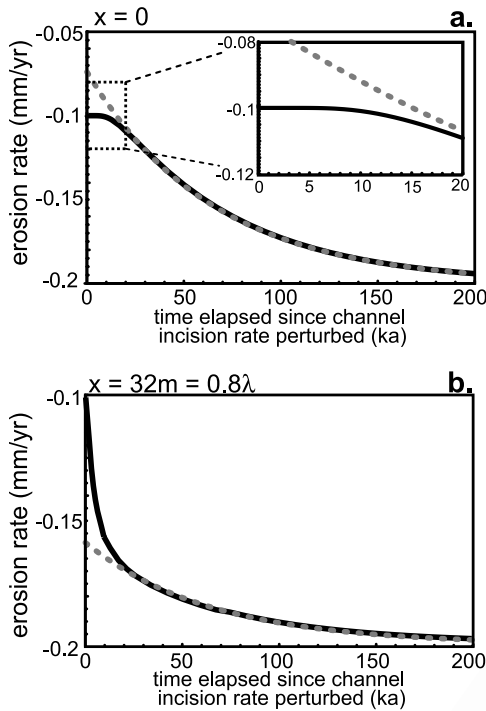


Figure 4. True erosion rate (solid lines) and erosion rate predicted by fitting equation (9) (dashed gray lines) as a function of time at (a) the divide ($x = 0$) and (b) a point near the channel ($x = 32 \text{ m} = 0.8\lambda$). The hillslope is the same as that described in Figure 3.

with higher wave numbers is to reduce the erosion rate near the divide (Figure 5a). This relative reduction in the erosion rate due to the harmonic functions with the higher numbers, and therefore more rapid response timescales, is what causes the delay in the response of the erosion rate at the divide (Figure 4a).

[19] The relative importance of individual harmonic functions, and therefore the relative importance of different response timescales (i.e., equation 10), may be determined by comparing the coefficients that multiply the time-varying exponential term in equation (8). We define a function:

$$M_E(n, x) = \frac{(-1)^n}{1 + 2n} \cos\left[\frac{(1 + 2n)\pi x}{2\lambda}\right] \sec\left[\frac{\pi x}{2\lambda}\right], \quad (11)$$

where M_E is the ratio of the coefficients that multiply the time varying exponential term of equation (8) for a wave number n to the coefficient when the wave number, n , is zero. In other words, M_E is defined by dividing the term within the summation in equation (8) with a wave number n by the term in the summation with n set to zero. By definition, M_E is equal to one when $n = 0$. For $n \neq 0$, M_E reflects the proportion of the erosion rate (M_E) signal that is contributed by the harmonic with wave number n . Because each harmonic function decays over the timescale described by equation (10), M_E measures the importance of higher harmonics ($n > 0$) while t is less than τ_n .

[20] The magnitude of the harmonics as a function of position is plotted in Figure 6. Recall from Figure 5 that if a

given harmonic takes a negative value, this causes a delayed response in the erosion rate. This corresponds to negative values of M_E , and as depicted in Figure 6 this effect is most pronounced near the divide ($x = 0$). Positive values of M_E indicate that fast moving signals are accelerating the response of the hillslope to the change in channel incision. This occurs in locations near the channel. Near the divide, the harmonic of $n = 1$ is a significant fraction of the total response of the hillslope (Figure 6). Because this harmonic is the principal cause of the delay between the time the channel incision rate is perturbed and the time the divide “feels” this signal, the time of delay can be estimated by the timescale of this harmonic. By equation (10), the delay in the response of the divide after the channel incision rate is perturbed is $\tau_0/9$. So, for example, in the hillslope depicted in Figures 3, 4, and 5, which has a length of 40 m and a diffusivity of $0.01 \text{ m}^2 \text{ yr}^{-1}$, τ_0 is approximately 65 ka, and τ_1 is approximately 7 ka. Examination of Figure 4b reveals that the divide begins responding to the transient incision signal at approximately 7 ka.

4. Timescales of Hillslope Response for Soil Thickness, Soil Production, and Hillslope Erosion Rate

[21] The analysis in sections 2 and 3 focuses on analytical solutions for idealized hillslopes where soil production and soil thickness are not considered. We now extend our

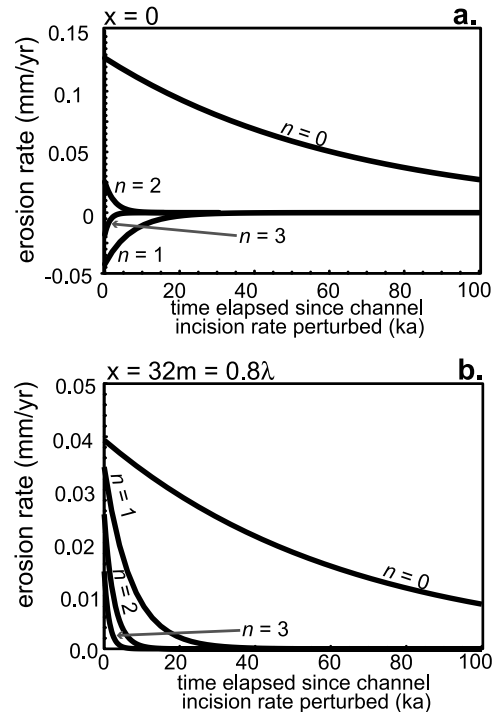


Figure 5. Erosion rate due to individual harmonics on a perturbed hillslope as a function of time. The symbol n refers to the wave number. (a) Harmonics at the divide ($x = 0$) and (b) harmonics at a point near the channel ($x = 32 \text{ m} = 0.8\lambda$). Note that the total erosion rate is the sum of all harmonics minus the perturbed incision rate I (see equation (8)).

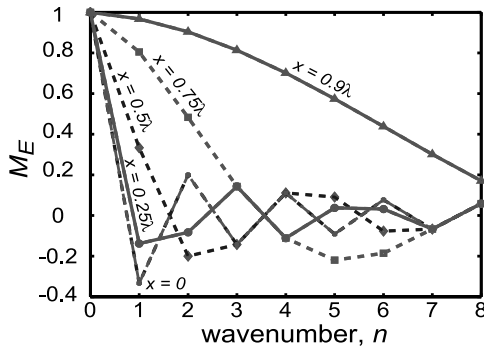


Figure 6. Values of M_E (see equation (11)) as a function of wave number.

358 analysis to include these and other factors. Returning to
 359 equations (2)–(4) to describe the soil-mantled hillslope, we
 360 assume that the soil may have a different dry bulk density
 361 than the soil (i.e., $\rho_s \neq \rho_\eta$). In addition, the soil production
 362 rate, p_η , is described by a function of the soil thickness
 363 (h). In several field locations [e.g., *Heimsath et al.*, 1997,
 364 2000, 2001], the soil production rate has been found to be
 365 a decreasing function of increasing soil thickness:

$$p_\eta = W_0 e^{-\frac{h}{\gamma}} \quad (12)$$

366 where W_0 ($L T^{-1}$) is the nominal rate of soil production
 367 when the soil thickness is zero and γ (L) is a length scale
 368 that characterizes the rate of decline in the soil production
 369 rate with increasing soil thickness. Others have argued for a
 370 soil production function that peaks at some intermediate soil
 371 thickness [*Ahnert*, 1976; *Anderson*, 2002; *Carson and*
 372 *Kirkby*, 1972; *Furbish and Fagherazzi*, 2001; *Wilkinson et al.*,
 373 2005]. Here we limit our analysis to a soil production
 374 function that takes the form of equation (12).

376 [22] Because the soil production as described by
 377 equation (12) is a nonlinear function of soil thickness,
 378 equations (2) and (4) are best solved numerically. In
 379 addition, the relationship between slope and sediment flux
 380 may be nonlinear. Examples include sediment flux that
 381 increases asymptotically as the hillslope approaches a
 382 critical gradient [*Andrews and Bucknam*, 1987; *Roering et al.*,
 383 1999, 2001, 2004], sediment flux that varies
 384 nonlinearly with slope due to biogenic effects [e.g., *Gabet*,
 385 2000; *Gabet et al.*, 2003; *Yoo et al.*, 2005], an effective
 386 sediment diffusivity that is a nonlinear function of soil
 387 thickness [*Anderson*, 2002], and sediment transport that is
 388 a function of the product of the hillslope gradient and the
 389 soil thickness [*Heimsath et al.*, 2005].

390 [23] For example, *Roering et al.* [2001] examined the
 391 adjustment timescale of hillslopes whose sediment flux was
 392 a nonlinear function of the hillslope gradient of the form

$$h\bar{v}_x = -D \frac{\partial \zeta}{\partial x} \left[1 - \left(\frac{1}{S_c} \frac{\partial \zeta}{\partial x} \right)^2 \right]^{-1}, \quad (13)$$

393 where S_c (dimensionless) is a critical slope. They found that
 394 the hillslopes experiencing sediment flux governed by

equation (13) had lower values of τ (see equation 9) than
 395 did hillslopes where sediment transport was a linear
 396 function of slope (e.g., equation 5). The response became
 397 more rapid (e.g., τ decreases) as hillslope gradients
 398 increased [*Roering et al.*, 2001]. Here we investigate the
 399 timescales of hillslope response as affected by the soil
 400 production and sediment flux that is proportional to the
 401 product of soil thickness and hillslope gradient.
 402
 403

4.1. Overview of Numerical Simulations

404
 [24] As we have demonstrated in section 2, changes in
 405 channel incision rates lead to signals that move away
 406 from the channels with different characteristic timescales
 407 (equation 10). We now concentrate on the timescale, τ , that
 408 may be extracted using equation (9) as described by
 409 *Howard* [1988] and *Roering et al.* [2001]. In each of our
 410 experiments, the function $F(t)$ in equation (9) is fit using
 411 least squares minimization with three properties of the
 412 hillslope soil at the divide: the erosion rate ($\partial \zeta_{bl}/\partial t$), the
 413 soil thickness (h), and the surface topography (ζ). We again
 414 note that when the time elapsed since the change in channel
 415 incision rate equals 3τ , the value of the soil property being
 416 analyzed (which could be topography, soil thickness, ero-
 417 sion rate, etc.) is within 5% of its final value if the new
 418 channel incision rate is steady in time. In our simulations,
 419 the most rapid incision rates (either I or I_0) were restricted to
 420 values less than W_0 so that none of the simulated hillslopes
 421 experienced zero soil thickness (in other words, the soil
 422 production rate could always keep up with the erosion rate).
 423

[25] Two sets of model runs were carried out. The model
 424 solves equations (2)–(4) using a finite difference scheme. In
 425 the first set of model runs, sediment transport was assumed
 426 to be a linear function of slope (equation (5)) and in the
 427 second set of model runs the sediment flux was assumed to
 428 be proportional to the product of the soil thickness and the
 429 hillslope gradient:
 430

$$h\bar{v}_x = -D_L h \frac{\partial \zeta_{bl}}{\partial x}, \quad (14)$$

where D_L is a transport coefficient of units $L T^{-1}$. We call
 431 equation (14) the depth-slope sediment flux law.
 432
 433

4.2. Linear Flux Law

434
 [26] Response timescales for hillslopes whose sediment
 435 flux is linearly proportional to slope are plotted in Figure 7.
 436 Figure 7a plots the ratio between the timescale extracted by
 437 equation (9) (τ) and the timescale τ_0 predicted as the long-
 438 term adjustment timescale by equation (10). This plot
 439 illustrates that the ratio between the density of the soil
 440 and the density of the soil's parent material can have a
 441 significant influence on the relaxation time of the hillslope.
 442 Figure 7b plots the ratio $\tau \bar{\rho}_s / \rho_\eta \tau_0$ (this ratio is equal to τ/τ_a ,
 443 see equation (15)) for the erosion rate and the soil thickness.
 444 These curves are approximately equal to one, such that the
 445 relaxation timescale of a hillslope where the dry bulk
 446 density of the soil is different from that of its parent material
 447 can be approximated by:
 448

$$\tau_a = \frac{4\rho_\eta \lambda^2}{\bar{\rho}_s \pi^2 D} \quad (15)$$

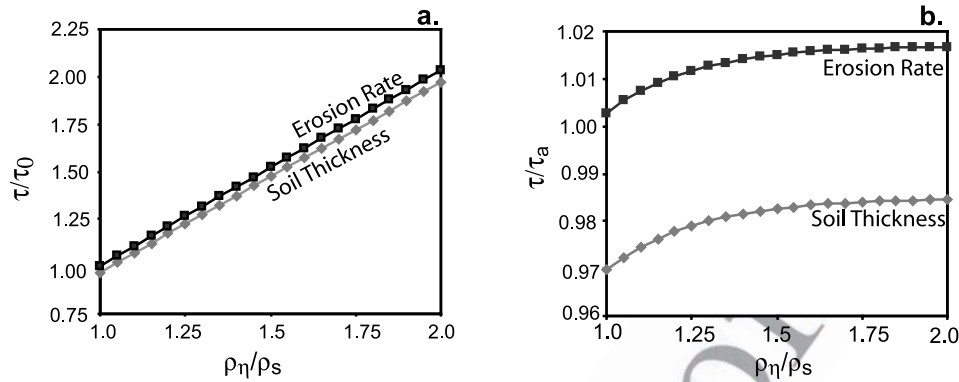


Figure 7. Plots of normalized (by (a) τ_0 and (b) τ_a) response timescale for the soil thickness and erosion rate. Other parameters from these model runs are $D = 0.005 \text{ m}^2 \text{ yr}^{-1}$, $\gamma = 0.3 \text{ m}$, $\lambda = 20 \text{ m}$, $W_0 = 0.0003 \text{ m yr}^{-1}$, $I_0 = -0.0001 \text{ m yr}^{-1}$, and $I = -0.0002 \text{ m yr}^{-1}$.

450 where τ_a is an approximate timescale of adjustment for
451 hillslopes that experience a linear sediment flux law and
452 experience soil production such that the hillslope is modeled
453 using equations (2)–(4) and (5).

454 [27] In Figure 8, we plot the difference between the
455 adjustment timescale τ extracted using equation (10) and
456 the approximated timescale τ_a , normalized by τ_a . As
457 observed by *Furbish and Fagherazzi* [2001] and *Mudd*
458 *and Furbish* [2005], soil thickness responds on a different
459 timescale than does the erosion rate (Figures 7b and 8a). In
460 addition, soil production also responds on a different
461 timescale, although the timescale of response for production
462 more closely matches that of erosion than does the soil
463 thickness. Our numerical experiments have shown that W_0
464 has a negligible influence on the timescale of hillslope
465 response, but both the ratio between the timescale of
466 response in the erosion rate and the timescale of response
467 of the soil thickness is sensitive to the difference between
468 the initial and final channel incision rates and also the length
469 scale (γ) over which soil production decays (Figure 8). The
470 length scale over which soil production decays is important
471 because it determines how sensitive the soil production rate
472 is to changes in soil depth.

473 [28] As the difference between the initial and final inci-
474 sion rates grows, the discrepancy between the approximate
475 timescale τ_a and the timescale of response of the hillslope τ
476 grows for the soil production rate, the erosion rate, and the
477 soil thickness. This effect is most pronounced for the soil
478 thickness, such that for hillslopes where there is a large
479 difference in the channel incision rates (e.g., $I/I_0 < 0.2$) the
480 response timescale of the soil thickness can be much greater
481 than the response timescale for the erosion rate (Figure 8a).
482 When channel incision rates are decreased, the soil thick-
483 ness responds to the change in channel incision more slowly
484 than the surface topography, whereas when the channel
485 incision rate increases the soil thickness adjusts more
486 rapidly than the hillslope erosion rate. As seen in Figure 8b,
487 the timescale of response will be more poorly predicted by
488 τ_a for thicker soils than for thinner soils (because γ sets the
489 soil thickness for a given erosion rate).

490 4.3. Depth-Slope Flux Law

491 [29] In the case of hillslopes where sediment flux is
492 governed by equation (14), τ_a is inappropriate for compar-

ing to the timescale, τ , which is measured by equation (9),
493 because D_L is of different units than D . Instead, the D in
494 equation (15) may be replaced by $D \sim D_L h$, which is
495 equivalent to stating that the diffusivity of the soil is depth
496 dependant [e.g., *Anderson*, 2002]. Figure 9 plots the ratio of
497 τ to this modified τ_a where in these plots $\tau_a = 4\rho_\eta \lambda^2 /$
498 $(\pi^2 D_L h \rho_s)$ and the soil thickness (h) is evaluated when this
499 thickness is in equilibrium with the lowest channel incision
500 rate (e.g., the slowest possible hillslope response timescale
501 for a given model run).
502

[30] Several features of response timescales for hillslopes
503 whose sediment flux is proportional to the product of the
504 soil thickness and the hillslope gradient contrast with hill-
505 slopes whose sediment flux is linearly proportional to slope.
506 In general, the response timescales of hillslopes with the
507 depth-slope sediment flux law deviate from the predicted
508 response timescale τ_a by a larger margin than do hillslopes
509 that experience the linear flux law. For some hillslopes
510 where the incision rate decreases ($I/I_0 < 1$) the predicted
511 response timescale (τ_a) is greater than the computed re-
512 sponse timescale (τ) although this may be an artifact of
513 selecting the τ_a based on the slowest possible response
514 timescale (e.g., calculating τ_a base on the minimum soil
515 thickness of the model run). For the hillslopes that experi-
516 ence and increased incision rate ($I/I_0 > 1$), the response
517 timescale increases for hillslopes that experience a flux law
518 that goes as the depth slope product. This contrasts with the
519 hillslopes that experience a linear flux law such that signals
520 from the channel can be stored in hillslopes that experience
521 sediment flux that is proportional to the depth slope product
522 for a much greater period of time than a similar hillslope
523 that experiences a linear sediment flux law.
524

525 5. Implications of Transient Response Timescales

[31] For a landscape that exhibits characteristics of being
528 in a transient state, for example, a landscape that has
529 widespread knickpoints within the fluvial network [e.g.,
530 *Arrowsmith et al.*, 1996; *Crosby and Whipple*, 2006], it is in
531 principle possible to extract information about the nature
532 and history of this transient condition from the state of the
533 hillslopes, including their geometry and soils [*Furbish*,
534 2003]. Examples of hillslope properties that may be usefully
535

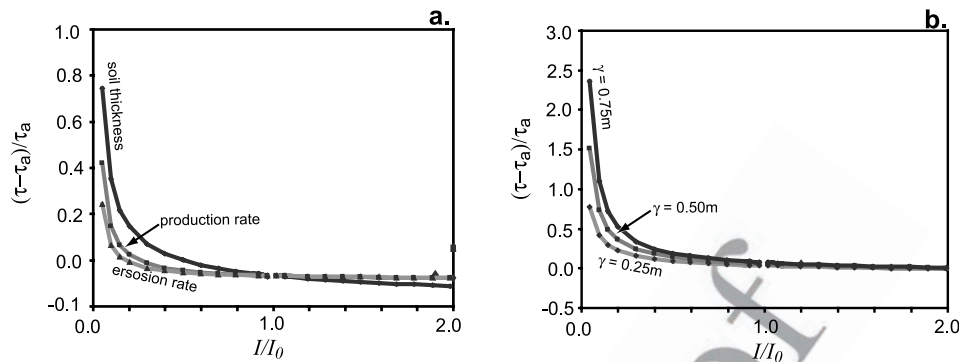


Figure 8. Difference between hillslope response timescale τ and approximate hillslope response timescale τ_a normalized by τ_a for hillslopes whose sediment flux is linearly proportional to the hillslope gradient. (a) Difference in response timescales for soil thickness, soil production rate, and erosion rate for a hillslope with parameters $\rho_r/\rho_s = 1.5$, $D = 0.005 \text{ m}^2 \text{ yr}^{-1}$, $\gamma = 0.25 \text{ m}$, $\lambda = 20 \text{ m}$, $W_0 = 0.0006 \text{ m yr}^{-1}$, and $I_0 = -0.0001 \text{ m yr}^{-1}$. (b) Normalized response timescale of soil thickness for different values of γ on a hillslope with parameters $\rho_r/\rho_s = 1.5$, $D = 0.005 \text{ m}^2 \text{ yr}^{-1}$, $\lambda = 20 \text{ m}$, $W_0 = 0.0006 \text{ m yr}^{-1}$, and $I_0 = -0.0001 \text{ m yr}^{-1}$. Note the change in scale on the vertical axes between Figures 8a and 8b. There are no data for $I/I_0 = 1$ because there is no change in the hillslope under these conditions.

536 measured are topography (obtained through topographic
537 surveys or laser altimetry [Shrestha *et al.*, 1999]), the spatial
538 distribution of soil thickness (obtained from soil pits or
539 ground penetrating radar [Neal, 2004]), and the spatial
540 distribution of soil production (obtained through cosmogenic
541 radionuclide dating techniques [Heimsath *et al.*, 1997]).
542 This point can be elaborated by considering implications
543 of the hillslope response timescale for two examples: (1) a
544 transient landscape for which the sediment flux law has
545 been constrained but the timing of the transient perturba-
546 tion to the fluvial network is unknown and (2) the timing
547 of the perturbation is known but the sediment flux law is
548 uncertain.

5.1. Known Flux Law, Unknown Timing of Transient Perturbation

551 [32] At present there are few examples of landscapes for
552 which the appropriate sediment flux law is known with
553 certainty, but methods are emerging by which this important
554 aspect of the landscape may be constrained [Anderson,
555 2002; Dietrich *et al.*, 2003; Furbish, 2003; Heimsath *et al.*,
556 2005]. Several authors have described methods for
557 providing relative ages of fault scarps or terraces [e.g.,
558 Andrews and Bucknam, 1987; Nash, 1980], but in many
559 cases absolute ages are preferable, and relative dating
560 techniques can only yield absolute ages when degradation
561 periods have been constrained for more than one hillslope
562 [Nash, 2005]. If, however, the sediment flux law is known,
563 then under ideal conditions an absolute (as opposed to
564 relative) time elapsed since the perturbation to the channel
565 incision rate may be estimated by measuring the erosion rate
566 along a hillslope profile and matching this information with
567 predictions of the hillslope response to a perturbation at its
568 base. For example, at a location where a step change in the
569 rate of channel incision is thought to have occurred, a point
570 on the hillslope can be selected (for example, the divide),
571 and the postulated history of soil production rate and soil
572 depth can be calculated numerically (generating information
573 similar to the time series of the erosion rate in Figure 4). The

measured and calculated soil depth and soil production rate
could then be matched to allow extraction of the time
elapsed since the step change in incision rate.

[33] For channel incision histories more complex than a
step change in incision rate, more sophisticated inversion
techniques would be required to constrain the history of
channel incision; these techniques are beyond the scope of
this contribution. We note, however, that transient perturba-
tions at one point in the channel network are thought to
propagate upstream [e.g., Whipple and Tucker, 1999].
Consider first several basins in which the timescales of
hillslope response are the same but the response of the
channel network to a perturbation in the channel incision
rate is different. As the changes in the channel incision rate
propagate upstream these incision signals leave a record

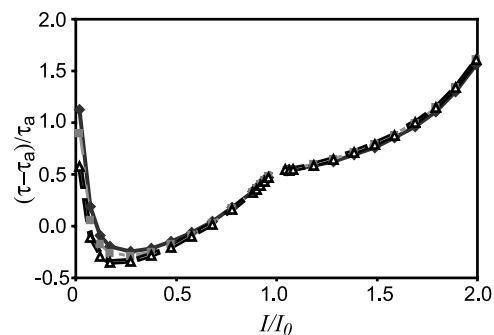


Figure 9. Difference between hillslope response timescale τ and approximate hillslope response timescale τ_a normalized by τ_a for hillslopes whose sediment flux is proportional to the hillslope gradient times the soil thickness. Diamonds represent the soil thickness, squares represent the production rate, and triangles represent the erosion rate. The hillslopes modeled have parameters $\rho_r/\rho_s = 1.5$, $D = 0.005 \text{ m}^2 \text{ yr}^{-1}$, $\gamma = 0.75 \text{ m}$, $\lambda = 20 \text{ m}$, $W_0 = 0.00025 \text{ m yr}^{-1}$, and $I_0 = -0.0001 \text{ m yr}^{-1}$. There are no data for $I/I_0 = 1$ because there is no change in the hillslope under these conditions.

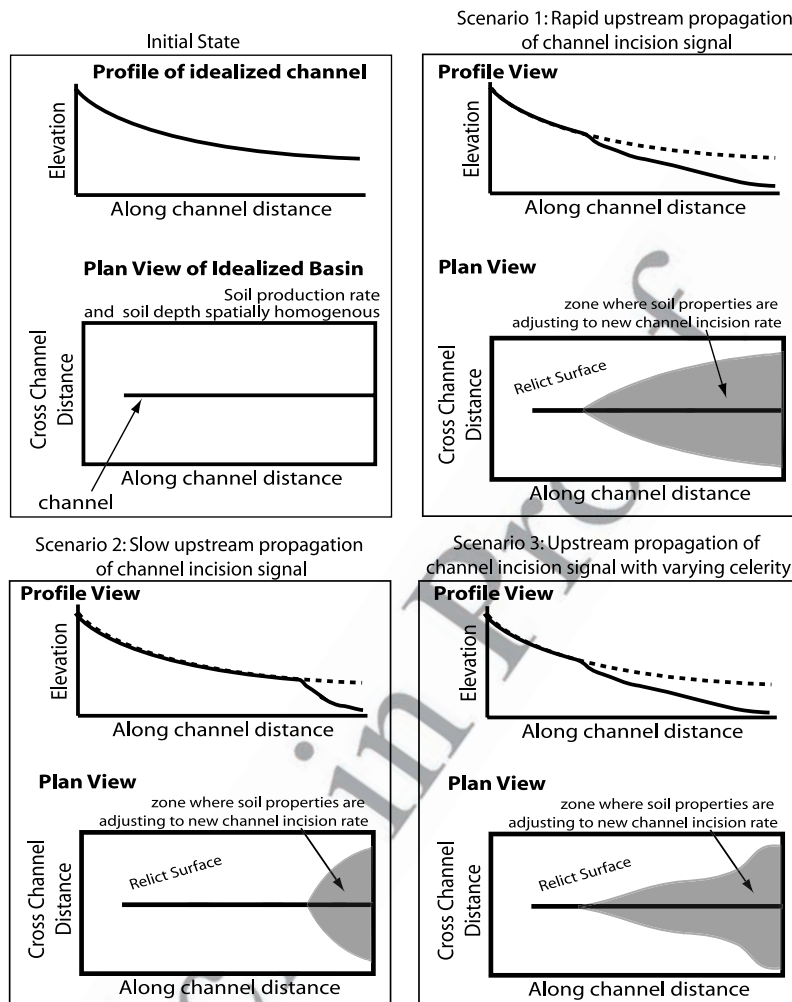


Figure 10. Schematic diagram showing idealized response of soil-mantled basin to transient channel incision rates. Prior to perturbation, the erosion rate of the basin is homogeneous, and likewise, the soil production rate and soil depth are homogeneous. Scenarios 1, 2, and 3 depict adjustment of the hillslope soils in the basin to different transient behaviors of the channel after the same time elapsed from the initial perturbation.

589 stored within the adjacent hillslope soils (Figure 10). The
 590 celerity at which a change in the channel incision rate
 591 propagates through the channel network will be reflected
 592 in the degree to which the perturbation of hillslope soil
 593 properties has advanced upslope away from the channel
 594 along the channel network. Thus measuring the extent to
 595 which the soil perturbation has advanced away from the
 596 channel as one moves through the drainage basin allows
 597 what is in essence a substitution of space for time, and can
 598 be indicative of the history of the celerity and magnitude of
 599 the channel incision signal (Figure 10, scenarios 1–3).

600 [34] Because hillslope soils respond to changes in channel
 601 incision rates, these soils provide a window into the past; if
 602 the incision rate in the channel has changed at some time in
 603 the past, surveying hillslope soil properties as one moves
 604 away from the channel is akin to reading a recorded history
 605 of the incision history of the channel. Moreover, of funda-
 606 mental importance is quantifying how long these disturban-
 607 ces remain imprinted on the landscape. The length of time
 608 that soil-mantled hillslopes may be used as recording devices

for channel incision histories is captured by the hillslope
 relaxation time and the fundamental timescales addressed in
 sections 2–4. Thus, in some cases hillslope soils may be
 used to quantify changes in channel incision rates for events
 that occurred a million years or more in the past.

[35] The hillslope response timescale may also be investi-
 gated based on the pattern of hillslope disturbance if the
 channel response to perturbation is known. In Figure 11 we
 show two different patterns of hillslope response to the
 same history of channel incision. The pattern of soil
 disturbance will reflect the speed of the hillslope response
 in relation to the celerity of the channel incision signal as it
 moves upstream if the channel incision history is the same
 in both basins (Figure 11). Thus different properties of a
 landscape as it responds to transient incision rates may be
 evaluated based on the existing information about the hill-
 slope response timescale. If the response timescale is
 known, the pattern of hillslope disturbance can be used to
 understand the spatial and temporal response of channel
 incision rates. If the channel incision history is known, on the

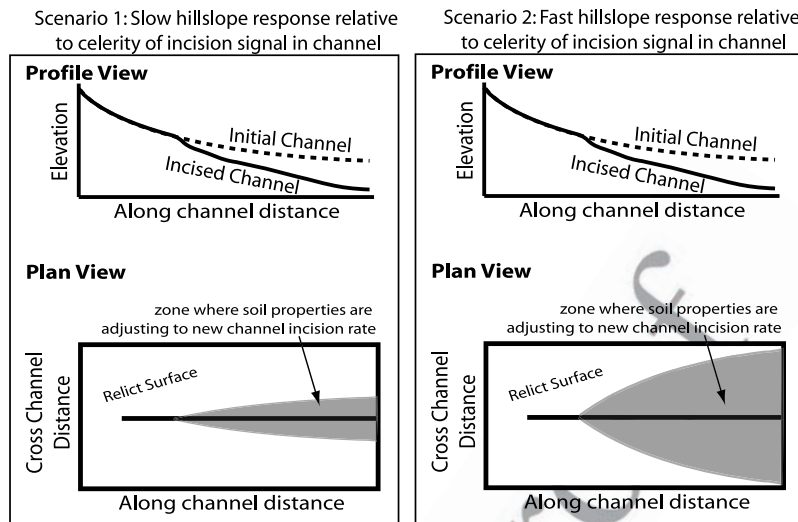


Figure 11. Schematic diagram showing idealized response of soil-mantled basin to transient channel incision rates (see text).

629 other hand, the pattern of hillslope response may be used to
 630 evaluate the relative speed of the hillslope response (and
 631 equivalently, the hillslope response timescale) to the celerity
 632 of the channel incision signal.

633 5.2. Known Timing of Transient Perturbation, 634 Unknown Flux Law

635 [36] In contrast to the situation described above, consider
 636 a landscape in which the sediment flux law is unconstrained
 637 but there is a known history of channel incision. Examples
 638 could include basins that drain into a body of water that
 639 both sets the base level for the basin and has a known
 640 history of relative elevation (e.g., by dated paleoshorelines
 641 or marine terraces), or a river system with dated strath
 642 terraces. As illustrated in section 4, hillslopes that have
 643 different sediment flux laws will respond differently to the
 644 same perturbation in the channel incision rate at their bases.
 645 A simple scenario consists of a step change in the channel
 646 incision rate. If the channel incision rate increases, a hill-
 647 slope involving a depth-slope product flux law requires a
 648 greater time to respond to this change in incision rate than
 649 does a hillslope involving a linear sediment flux law. The
 650 implication is that if a soil property such as the soil
 651 production rate is measured at the divide at a known time
 652 following the step change in channel incision rate, then this
 653 soil property must simultaneously be compatible with the
 654 new channel incision rate and with the “correct” sediment
 655 flux law, among alternatives. That is, because different
 656 sediment flux laws have different characteristic timescales
 657 of adjustment to changes in the channel incision rate at the
 658 base of a hillslope, different sediment flux laws will produce
 659 different spatial patterns of hillslope soil properties that may
 660 be used to constrain the appropriate flux law [Furbish,
 661 2003; Roering *et al.*, 2004].

663 6. Conclusions

664 [37] Channel incision drives the evolution of humid soil-
 665 mantled hillslopes. When channel incision rates change, soil
 666 response signals from such changes propagate away from

the channel. These signals operate on a number of time- 667
 scales. We have demonstrated that for soil-mantled hill- 668
 slopes two timescales are particularly important. The first 669
 timescale, which we call τ_0 , determines how much time 670
 must pass after a change in the channel incision rate before 671
 the entire hillslope equilibrates to this new condition. For 672
 hillslopes that experience sediment flux that is linearly 673
 proportional to slope and whose soil is the same density 674
 as the material from which the soil is derived, this timescale 675
 is approximated by $4\lambda^2/(\pi^2 D)$ where λ is the length of the 676
 hillslope and D is the sediment diffusivity. At a time of $3\tau_0$ 677
 after a perturbation on the channel incision rate, the topog- 678
 raphy and erosion rate of the hillslope are within 5% of their 679
 final values, and the hillslope can be reasonably considered 680
 to be at steady state. An additional timescale is the time it 681
 takes a signal caused by a change in the channel incision 682
 rate to propagate from the channel to the divide. This 683
 timescale is approximated by $\tau_0/9$. 684

[38] As described by both Furbish [2003] and Roering *et* 685
al. [2004], measurement of several spatially and temporally 686
 varying soil properties can be used to constrain the dynamic 687
 response of hillslopes to changes in the channel incision 688
 rate. The strongest spatial variation in soil properties can be 689
 expected to occur within the time after channel perturbation 690
 of $0 < t < \tau_0/9$, when the hillslope near the channel has 691
 begun to adjust to the new channel incision rate but the 692
 divide has not yet “felt” this disturbance. 693

[39] On hillslopes where soil is not the same density as 694
 the material from which the soil is derived (i.e., when $\rho_s \neq$ 695
 ρ_η), the ratio between the two densities is of first-order 696
 importance in determining the hillslope response to a 697
 change in the channel incision rate. In this case, the 698
 response timescale can be approximated by $4\rho_\eta\lambda^2/(\pi^2 D\rho_s)$ 699
 if sediment flux is linearly proportional to slope. The 700
 difference in the adjustment timescales for soil thickness 701
 and soil erosion rate is sensitive to the ratio between the 702
 initial channel incision rate (I_0) and the channel incision rate 703
 after it has been perturbed (I). 704

[40] For hillslopes where sediment transport is linearly 705
 proportional to slope, the difference in the adjustment 706

707 timescales for soil thickness and soil erosion rate is greater
 708 for hillslopes where the new incision rate I is a smaller
 709 proportion of the old incision rate I_0 , whereas on hillslopes
 710 where the sediment flux is proportional to the depth slope
 711 product accelerated incision results in increased response
 712 timescales. Because hillslopes with different sediment flux
 713 laws respond to changes in channel incision on different
 714 timescales, it is critical to correctly identify the flux law
 715 operating on a soil-mantled landscape if one is to determine
 716 if a hillslope is approaching a steady state condition at some
 717 known time after a channel incision event. This identifica-
 718 tion of the correct flux law is also critical if one is to assess
 719 the duration that signals (such as topography, soil thickness,
 720 soil production rates, and erosion rates) from transient
 721 erosion events will be stored in hillslope soils.

722 Notation

D	sediment diffusivity ($L^2 T^{-1}$).
η	elevation of soil-bedrock boundary (L).
γ	soil production decay length scale (L).
h	soil thickness (L).
I, I_0	channel incision rate and initial incision rate, respectively ($L T^{-1}$).
λ	length of the hillslope (L).
M_E	ratio determining the magnitude of the time vary component of the erosion rate as a function of position and wave number.
n	wave number (dimensionless).
p_η	soil production rate ($L T^{-1}$).
$\bar{\rho}_s$	depth averaged dry bulk density of hillslope soil ($M L^{-3}$).
ρ_η	Dry bulk density of parent material ($M L^{-3}$).
S_c	critical slope for linear-critical flux law (dimensionless).
t	time (T).
τ	decay timescale (T).
τ_a	approximate hillslope response timescale for hillslopes where $\rho_s \neq \rho_\eta$.
τ_n	decay timescale for individual harmonic functions with wave number n .
\bar{v}_x	depth averaged sediment velocity in the x direction ($L T^{-1}$).
W_0	nominal rate of soil production ($L T^{-1}$).
x	distance from the divide (L).
ζ	elevation of soil surface (L).
ζ_{bl}	elevation of soil surface relative to the channel (L).

774 [41] **Acknowledgments.** This work was supported by the National
 775 Science Foundation (EAR-0125843). The comments of Josh Roering,
 776 Jaakko Putkonen, and an anonymous reviewer helped to refine this
 777 contribution.

778 References

779 Ahnert, F. (1976), Brief description of a comprehensive three-dimensional
 780 process-response model of landform development, *Z. Geomorph. Suppl.*,
 781 25, 29–49.
 782 Ahnert, F. (1987), Approaches to dynamic equilibrium in theoretical simula-
 783 tions of slope development, *Earth Surf. Processes Landforms*, 12(1), 3–15.
 784 Anderson, R. S. (2002), Modeling the tor-dotted crests, bedrock edges, and
 785 parabolic profiles of high alpine surfaces of the Wind River Range,
 786 Wyoming, *Geomorphology*, 46(1–2), 35–58.
 787 Andrews, D. J., and R. C. Bucknam (1987), Fitting degradation of shoreline
 788 scarps by a nonlinear diffusion model, *J. Geophys. Res.*, 92(B12),
 789 12,857–12,867.

Arrowsmith, J. R., D. D. Pollard, and D. D. Rhodes (1996), Hillslope 790
 development in areas of active tectonics, *J. Geophys. Res.*, 101(B3), 791
 6255–6275.
 Carslaw, H. S., and J. C. Jaeger (1959), *Conduction of Heat in Solids*, 510 793
 pp., Oxford Univ. Press, New York. 794
 Carson, M. A., and M. J. Kirkby (1972), *Hillslope Form and Process*, 475 795
 pp., Cambridge Univ. Press, New York. 796
 Crosby, B. T., and K. X. Whipple (2006), Knickpoint initiation and distri- 797
 bution within fluvial networks: 236 waterfalls in the Waipaoa River, 798
 North Island, New Zealand, *Geomorphology*, 82(1–2), 16–38. 799
 Culling, W. E. H. (1960), Analytical theory of erosion, *J. Geol.*, 68, 336– 800
 344. 801
 Culling, W. E. H. (1963), Soil creep and the development of hillside slopes, 802
J. Geol., 71, 127–161. 803
 Culling, W. E. H. (1965), Theory of erosion on soil-covered slopes, 804
J. Geol., 73, 230–254. 805
 Davis, W. M. (1899), The geographical cycle, *Geogr. J.*, 14, 481–504. 806
 Deen, W. M. (1998), *Analysis of Transport Phenomena*, 597 pp., Oxford 807
 Univ. Press, New York. 808
 Dietrich, W. E., D. G. Bellugi, L. S. Sklar, and J. D. Stock (2003), Geo- 809
 morphic transport laws for predicting landscape form and dynamics, in 810
Prediction in Geomorphology, Geophys. Monogr. Ser., vol. 135, edited by 811
 P. R. Wilcock and R. M. Iverson, pp. 103–132, AGU, Washington, D. C. 812
 Fernandes, N. F., and W. E. Dietrich (1997), Hillslope evolution by diffu- 813
 sive processes: The timescale for equilibrium adjustments, *Water Resour.* 814
Res., 33(6), 1307–1318. 815
 Furbish, D. J. (2003), Using the dynamically coupled behavior of the land- 816
 surface geometry and soil thickness in developing and testing hillslope 817
 evolution models, in *Prediction in Geomorphology, Geophys. Monogr.* 818
Ser., vol. 135, edited by P. R. Wilcock and R. M. Iverson, pp. 169–182, 819
 AGU, Washington, D. C. 820
 Furbish, D. J., and S. Fagherazzi (2001), Stability of creeping soil and 821
 implications for hillslope evolution, *Water Resour. Res.*, 37(10), 2607– 822
 2618. 823
 Gabet, E. J. (2000), Gopher bioturbation: Field evidence for non-linear 824
 hillslope diffusion, *Earth Surf. Processes Landforms*, 25(13), 1419– 825
 1428. 826
 Gabet, E. J., O. J. Reichman, and E. W. Seabloom (2003), The effects of 827
 bioturbation on soil processes and sediment transport, *Annu. Rev. Earth* 828
Planet. Sci., 31, 249–273. 829
 Gilbert, G. K. (1877), *Report on the Geology of the Henry Mountains*, 160 830
 pp., U.S. Geol. Surv., Reston, Va. 831
 Gilbert, G. K. (1909), The convexity of hilltops, *J. Geol.*, 17, 344–350. 832
 Hack, J. T. (1960), Interpretation of erosional topography in humid temper- 833
 ate region, *Am. J. Sci.*, 258-A, 80–97. 834
 Heimsath, A. M., W. E. Dietrich, K. Nishiizumi, and R. C. Finkel (1997), 835
 The soil production function and landscape equilibrium, *Nature*, 836
 388(6640), 358–361. 837
 Heimsath, A. M., J. Chappell, W. E. Dietrich, K. Nishiizumi, and R. C. 838
 Finkel (2000), Soil production on a retreating escarpment in southeastern 839
 Australia, *Geology*, 28(9), 787–790. 840
 Heimsath, A. M., J. Chappell, W. E. Dietrich, K. Nishiizumi, and R. C. 841
 Finkel (2001), Late Quaternary erosion in southeastern Australia: A field 842
 example using cosmogenic nuclides, *Quat. Int.*, 83(5), 169–185. 843
 Heimsath, A. M., J. Chappell, N. A. Spooner, and D. G. Quetiaux (2002), 844
 Creeping soil, *Geology*, 30(2), 111–114. 845
 Heimsath, A. M., D. J. Furbish, and W. E. Dietrich (2005), The illusion of 846
 diffusion: Field evidence for depth-dependent sediment transport, *Geol-* 847
ogy, 33(12), 949–952. 848
 Howard, A. D. (1988), Equilibrium models in geomorphology, in *Modeling* 849
in Geomorphic Systems, edited by M. G. Anderson, pp. 49–72, John 850
 Wiley, Hoboken, N. J. 851
 Jyotsna, R., and P. K. Haff (1997), Microtopography as an indicator of 852
 modern hillslope diffusivity in arid terrain, *Geology*, 25(8), 695–698. 853
 King, L. C. (1953), Canons of landscape evolution, *Geol. Soc. Am. Bull.*, 854
 64, 721–752. 855
 Kirkby, M. J. (1967), Measurement and theory of soil creep, *J. Geol.*, 75(4), 856
 359–378. 857
 Mudd, S. M., and D. J. Furbish (2004), Influence of chemical denudation 858
 on hillslope morphology, *J. Geophys. Res.*, 109, F02001, doi:10.1029/ 859
 2003JF000087. 860
 Mudd, S. M., and D. J. Furbish (2005), Lateral migration of hillcrests in 861
 response to channel incision in soil-mantled landscapes, *J. Geophys. Res.*, 862
 110, F04026, doi:10.1029/2005JF000313. 863
 Mudd, S. M., and D. J. Furbish (2006), Using chemical tracers in hillslope 864
 soils to estimate the importance of chemical denudation under conditions 865
 of downslope sediment transport, *J. Geophys. Res.*, 111, F02021, 866
 doi:10.1029/2005JF000343. 867
 Nash, D. B. (1980), Morphologic dating of degraded normal-fault scarps, 868
J. Geol., 88(3), 353–360. 869

- 870 Nash, D. B. (2005), A general method for morphologic dating of hillslopes,
871 *Geology*, 33(8), 693–695. 897
- 872 Neal, A. (2004), Ground-penetrating radar and its use in sedimentology:
873 Principles, problems and progress, *Earth Sci. Rev.*, 66(3–4), 261–330. 898
- 874 Paola, C., and V. R. Voller (2005), A generalized Exner equation for sedi-
875 ment mass balance, *J. Geophys. Res.*, 110, F04014, doi:10.1029/
876 2004JF000274. 900
- 877 Penck, W. (1972), *Morphological Analysis of Land Forms: A Contribution*
878 *to Physical Geology*, reprint ed., translated from German by H. Czech and
879 K. Cumming Boswell, 429 pp., Hafner, New York. 901
- 880 Roering, J. J. (2004), Soil creep and convex-upward velocity profiles:
881 Theoretical and experimental investigation of disturbance-driven sedi-
882 ment transport on hillslopes, *Earth Surf. Processes Landforms*, 29(13),
883 1597–1612. 902
- 884 Roering, J. J., J. W. Kirchner, and W. E. Dietrich (1999), Evidence for
885 nonlinear, diffusive sediment transport on hillslopes and implications
886 for landscape morphology, *Water Resour. Res.*, 35(3), 853–870. 903
- 887 Roering, J. J., J. W. Kirchner, and W. E. Dietrich (2001), Hillslope evolu-
888 tion by nonlinear, slope-dependent transport: Steady state morphology
889 and equilibrium adjustment timescales, *J. Geophys. Res.*, 106(B8),
890 16,499–16,513. 904
- 891 Roering, J. J., P. Almond, P. Tonkin, and J. McKean (2002), Soil transport
892 driven by biological processes over millennial time scales, *Geology*,
893 30(12), 1115–1118. 905
- 894 Roering, J. J., P. Almond, P. Tonkin, and J. McKean (2004), Constraining
895 climatic controls on hillslope dynamics using a coupled model for
896 the transport of soil and tracers: Application to loess-mantled
hillslopes, South Island, New Zealand, *J. Geophys. Res.*, 109, F01010, 897
doi:10.1029/2003JF000034. 898
- Shrestha, R. L., W. E. Carter, M. Lee, P. Finer, and M. Sartori (1999),
Airborne laser swath mapping: Accuracy Assessment for surveying and
mapping applications, *J. Am. Congr. Surv. Mapp.*, 59(2), 83–94. 900
- Whipple, K. X., and G. E. Tucker (1999), Dynamics of the stream-power
river incision model: Implications for height limits of mountain ranges,
landscape response timescales, and research needs, *J. Geophys. Res.*,
104(B8), 17,661–17,674. 902
- Wilkinson, M. T., J. Chappell, G. S. Humphreys, K. Fifield, B. Smith, and
P. Hesse (2005), Soil production in heath and forest, Blue Mountains,
Australia: Influence of lithology and palaeoclimate, *Earth Surf. Processes*
Landforms, 30(8), 923–934. 906
- Yoo, K., R. Amundson, A. M. Heimsath, and W. E. Dietrich (2005), Pro-
cess-based model linking pocket gopher (*Thomomys bottae*) activity to
sediment transport and soil thickness, *Geology*, 33(11), 917–920. 911
- Young, A. (1978), A twelve-year record of soil movement on a slope,
Z. Geomorph. Suppl., 29, 104–110. 912
- D. J. Furbish, Department of Earth and Environmental Sciences, 915
Vanderbilt University, Nashville, TN 37235, USA. 917
- S. M. Mudd, Department of Civil and Environmental Engineering, 918
Vanderbilt University, Nashville, TN 37235, USA. (simon.m.mudd@ 919
vanderbilt.edu) 920